Telechelic Poly(*N*-isopropylacrylamide): Polymerization and Chain Aggregation in Solution

Dennis W. Smithenry,† Mun-Sik Kang,‡ and Vinay K. Gupta*,‡

Departments of Chemistry and Chemical Engineering, University of Illinois, Urbana−Champaign, 600 S. Mathews Avenue, Urbana, Illinois 61801

Received May 4, 2001; Revised Manuscript Received August 24, 2001

ABSTRACT: The synthesis of telechelic poly(*N*-isopropylacrylamide) (PNIPAM) with carboxylic acid termini was accomplished using the primary radical termination mechanism. Polymers with molecular weight (M_n) ranging from 32 to 5 kDa could be prepared by changing the monomer-to-initiator ratio and the time of polymerization. Modeling of the polymerization by a simple kinetic model based on radical initiation, propagation, and primary radical termination by initiator was performed. Prediction of the molecular weights by this model showed good agreement with the experimentally observed values. Characterization of the polymer revealed a complex aggregation phenomena in DMF solutions at temperatures of 60−70 °C. For samples with M_n between 8.3 and 12.2 kDa the presence of nanometer size aggregates was evident in the elution chromatogram, and the laser light scattered at right angles. It was found that the aggregation appeared at a polymer concentration that was far below the overlap concentration of the polymer chains, and the aggregates could not be broken up by either dilution of the solutions or addition of lithium bromide to DMF. The solvent was found to play a role, and aggregation was observed in another polar solvent such as *N*-methylpyrollidone but not in a nonpolar solvent such as tetrahydrofuran.

Introduction

Stimuli-sensitive polymers that respond to external fields such as pH, temperature, and light are of great interest for active control of properties of surfaces and solutions. In this arena, poly(*N*-isopropylacrylamide) (PNIPAM) has been the focus of significant attention because of its thermoresponsive properties.[1−4] Past studies have demonstrated that aqueous solutions of PNIPAM exhibit a lower critical solution temperature (LCST) around 32 °C.[5] Dehydration of polymer chains upon heating causes a coil-to-globule transition and produces thermoreversible phase separation in solutions and changes in the hydrophilic nature of surfaces modified with PNIPAM.[4] Recent studies have exploited these phenomena for applications in drug delivery,[6] separations,[2,7−9] energy transduction,[10] and catalysis.[11]

In the context of a larger research framework we have focused on the synthesis of telechelic PNIPAM, its properties, and its uses in bulk solutions and on surfaces. Telechelics carry functional groups at both ends of the polymer chain and are immensely useful in industry as precursors for block, graft, and cross-linked polymers.[12] Associating telechelic polymers are of technological importance in viscosity modification, cosmetics, water treatment, and oil recovery.[13] Past studies have also reported diverse uses of telechelics in peptide synthesis, enzyme modification, and binders for solid rocket propellant.[14] Consequently, a variety of synthetic approaches have been investigated for preparing telechelics with different functionalities and a controlled molecular weight distribution.[12,15] In the case of PNIPAM, Takei and co-workers[9,16] recently showed that free radical oligomerization with a chain transfer agent such as mercaptopropionic acid can be used to prepare semi-telechelic binders for PNIPAM oligomers that possesses carboxylic acid functionality on one end of the polymer chain. The semi-telechelic PNIPAM then enables the introduction of temperature responsive functions to biomolecules such as enzyme, antigens, antibodies, and nucleotides by facile conjugation to the biomolecules via the carboxylic acid end group.[3,8,9,16,17]

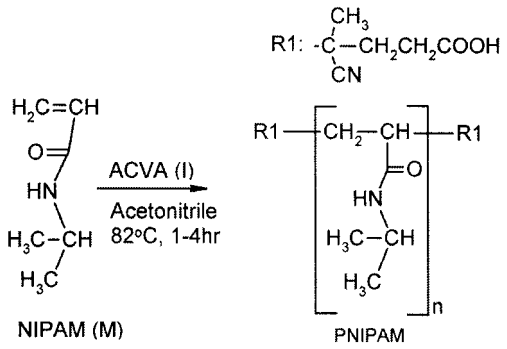

Figure 1. Schematic of the synthesis of telechelic PNIPAM.

In this paper we report the synthesis and characterization of telechelic PNIPAM wherein the polymer chain possesses carboxylic acid groups on both ends. We show that a telechelic structure for PNIPAM can be obtained by using a synthetic approach (Figure 1) that relies on primary radical termination mechanism.[18] We demonstrate that the molecular weight of the telechelic PNIPAM can be manipulated by changing the relative ratio of the monomer to the initiator and discuss the kinetics of polymerization by comparing experimental results with the predictions of a simple model. Characterization of the telechelic PNIPAM using right angle light scattering, viscometry, and size-exclusion chromatography reveals an anomalous aggregation phenomena in dimethylformamide (DMF).

Experimental Section

Chemicals. All reagents, unless otherwise noted, were purchased from Aldrich Chemicals (Milwaukee, WI) and used

† Department of Chemistry.
‡ Department of Chemical Engineering.
* To whom correspondence should be addressed. E-mail vgupta@uiuc.edu; Fax 217-333-5052; Tel 217-244-2247.

10.1021/ma010769b CCC: $20.00
Published on Web 10/18/2001

without further purification. 4,4′-Azobis(4-cyanovaleric acid) initiator (ACVA) used in this study was purchased from Fluka Chemical Corp. (Milwaukee, WI) and used as received. The solvents used in this study—hexane, acetonitrile, and DMF (Fisher)—were of reagent grade. Purified water was from an EasyPure UV system (Barnstead, IA).

Preparation of Telechelic Poly(isopropylacrylamide). *N*-Isopropylacrylamide (NIPAM) monomer was recrystallized in hexane, and a 0.25 M solution of NIPAM in acetonitrile was used for all reactions. The volume of acetonitrile that was used varied from 56.4 to 177 mL over the different polymerization reactions reported in this paper. The NIPAM solution was placed in a 250 mL three-necked round-bottom flask and bubbled with nitrogen for 30 min. The flask was then placed in an oil bath heated to 82 ± 2 °C for at least 10 min. Subsequently, solid ACVA initiator was quickly added to the flask starting the reaction time. The ratio of initiator to monomer ($P = 100[I]_0/[M]_0$) was varied from 1 to 9%, and the reaction time (t_{rxn}) was varied from 1 to 4 h (see Results and Discussion). After polymerization was completed the flask was removed from the heated oil bath.

The clear reaction mixture contained PNIPAM, unreacted NIPAM monomer, and ACVA in acetonitrile. The solvent was removed by vacuum evaporation and by heating to 45−50 °C. The separated solid was subsequently dissolved in a minimum amount of pure water. Typically a 4−5 wt % solution was found to fully dissolve under extensive cooling (∼0 °C). The aqueous solution was dialyzed in flowing water for 1−3 days to remove the low-molecular-weight monomer and ACVA impurities. All but one sample were dialyzed using a Spectra/Por membrane with a molecular weight cutoff (MWCO) of 1000. A snakeskin membrane (Pierce Chemicals, Rockford, IL) with MWCO = 3500 was used for the sample where $P = 1\%$ and $T = 1$ h.

Following dialysis, the solution was transferred to centrifuge tubes and heated to 50 °C for 10 min. A white precipitate was observed to form immediately upon heating. The samples were centrifuged for 1 h at 9000 rpm at a temperature of 38 °C. The solid precipitate was collected and dried in a vacuum oven at a temperature of 60 °C for 24 h or more to remove any remaining water.

Characterization of PNIPAM. Molecular weight and intrinsic viscosity ([η]) characterization was performed on a Viscotek model 300 triple detector array (TDA). The column was calibrated with narrow polystyrene standards ranging from 1 to 1850 kDa. DMF with 0.05 M LiBr at 60 °C served as the mobile phase. A 0.2 μm filter was used to filter the solutions prior to injection in the column. In the TDA system, signals are measured in tandem from a refractometer (RI) to estimate mass concentration, a photodetector to estimate intensity of laser light scattered at 90° (RALLS), and a four-capillary viscometer to estimate the viscosity (VISC). The SEC^3 method[19] uses these three signals to determine M_w, M_n, [η], and R_g. Details and evaluation of the triple detector method are available in the literature.[19,20]

To measure the concentration of acid groups per PNIPAM chain, the polymer was analyzed via titration. A known mass of PNIPAM was diluted in approximately 15 mL of water and titrated with 0.0144 M NaOH. The pH measurements were carried out with a benchtop pH meter (model 59003-10, Cole Palmer, IL). Cloud point measurements were performed for 0.5 wt % aqueous solutions of the various PNIPAM products using a right-angle light scattering turbidometer (model DT1000, HF Instruments, Inc.). The solution's temperature was controlled via a water-circulated custom cell holder. The turbidity of the solution was measured as the temperature was increased in ∼1 °C steps. At each step, the temperature was stabilized for 10 min before measurement of turbidity.

Results and Discussion

Polymerization and Structural Characterization. To characterize the structure of the telechelic PNIPAM and to compare the experimental results with a kinetic model of the polymerization, molecular weight measurements for the PNIPAM were carried out on a gel chromatography column equipped with three detectors. The values of M_n and M_w estimated by the SEC^3 method indicated that the samples had low polydispersity (<1.5), which was inconsistent with the width of the RI chromatogram and the polydispersity in apparent molecular weights determined from ordinary SEC calculation. The lower polydispersity from SEC^3 was, plausibly, a result of higher estimates of M_n. The RALLS signal, which is proportional to the product of concentration and molecular weight, underestimated the contribution of low-molecular-weight species. This problem in light scattering signal was also exacerbated by the small optical contrast between PNIPAM and DMF.

Table 1. Molecular Weight Characteristics of Telechelic PNIPAM

PNIPAM sample	P ($100[I_2]_0/[M]_0$)	T_{rxn} (h)	M_n[a] (kDa)	M_w[a] (kDa)	R_{COOH}	$C[\eta]$, deg of chain overlap
P1T1	1	1	32.3	57.7	2.8	0.08
P1T4	1	4	21.7	36.6	2.0	0.06
P3T1	3	1	10.5	20.5	2.5	0.02
P3T4	3	4	7.8	17.5	2.2	0.01
P5T1	5	1	12.2	19.8	2.6	0.01
P5T2	5	2	6.8	16.5	1.9	0.01
P5T3	5	3	6.7	15.3	2.3	0.01
P5T4	5	4	5.1	14.4	1.8	0.01
P9T1	9	1	8.3	16.5	1.8	0.01
P9T4	9	4	6.5	13.9	2.1	0.02

[a] Mark−Houwink parameters in $[\eta] = KM^a$ where $\log K_{PS} = -3.5637$, $a_{PS} = 0.599$, $\log K_{PNIPAM} = -4.78 \pm 0.51$, and $a_{PNIPAM} = 0.79 \pm 0.11$.

Molecular weights M_n and M_w (Table 1) were, therefore, obtained from the polystyrene equivalent apparent molecular weight by using Mark−Houwink parameters (K, a) that were determined from viscometric data for both PS and PNIPAM in DMF at 60 °C. Several trends can be observed in M_n and M_w (Table 1) as the ratio of initiator-to-monomer concentration ($P = 100[I_2]_0/[M]_0$) and reaction time for the polymerization were changed. Qualitatively, a high initiator concentration was expected to lead to an increase in the amount of termination of growing polymer chains and result in shorter chains. The data in Table 1 show that both M_n and M_w decreased as the initiator concentration increased from 1% to 9%. Both M_n and M_w also decreased with an increase in reaction time. Qualitatively, this can be interpreted in terms of less monomer becoming available for polymerization and thereby leading to shorter polymer chains. The polydispersity index of all the dialyzed samples was relatively constant, implying that a similar range of polymer chain lengths was produced as the polymerization progressed. The phase separation behavior of the polymer in aqueous solutions at the LCST was characterized by cloud point measurements. While cloud point measurements do not represent the most precise determination of LCST, past studies have found that the cloud point correlates quite well with the LCST.[4] All the polymers in Table 1 showed a cloud point between 29 and 31 °C. Even though the materials were not monodisperse, a slight molecular weight dependence could be discerned, and the samples with the highest molecular weight generally exhibited a rise in the turbidometer signal between 29 and 30 °C. This trend is consistent with past studies of LCST wherein it has been reported that LCST decreases with increase in molecular weight.[21]

To determine whether the PNIPAM had a telechelic structure, a standard titration was performed on each sample to assess the number of carboxylic acid end groups introduced by ACVA during initiation and termination of the polymer chain. The carboxylic acid per chain (R_{COOH}) ratio (Table 1) averaged over all samples was 2.2 ± 0.3. Several factors contribute to the variance in R_{COOH}. The ratio R_{COOH} is affected by errors in determination of M_n, especially for low-molecular-weight samples and the presence of semi-telechelic polymer chains that did not undergo termination by the PRT. Even though we dialyzed the samples for a long time, it is plausible that traces of unreacted ACVA were trapped in the polymer and influenced the titration.[22] However, the average carboxylic acid ratio value close to 2 suggests that the majority of polymer chains in each sample possess a telechelic structure.

To simulate the polymerization, we used a simple kinetic model based on decomposition of the initiator into radicals, initiation of polymer chains by the radicals, propagation of chains by addition of monomer, and termination by initiator radicals.[23] Under assumptions of equal reactivity regardless of size of propagating radicals, negligible chain transfer to the solvent, and steady state for the concentration of free radicals in the system, it has been shown[24] that primary radical termination leads to a rate of polymerization that is

$$R_p = \frac{d[M(t)]}{dt} = -k_{poly}[M(t)]^2$$

where k_{poly} is a polymerization rate constant. The change in monomer concentration as a function of time is then

$$\frac{1}{[M(t)]} = \frac{1}{[M]_0} + k_{poly}t$$

Combining above with a first-order decomposition of the initiator gives the average kinetic chain length

$$DP(t) \cong \frac{R_p}{R_i} = \frac{k_{poly}[M(t)]^2}{2fk_D[I_2]_0 \exp(-k_D t)}$$

where k_D is the ACVA decomposition rate constant. If $P = 100[I_2]_0/[M]_o$ is the percentage ratio of initiator to monomer added at the beginning of the polymerization reaction, then

$$DP(t) = \frac{50k_{poly}[M]_0}{fk_D P(1 + k_{poly}[M]_0 t)\exp(-k_D t)}$$

Here f is the fraction of the initiator radicals produced that initiate polymerization.

To perform a kinetic simulation of the polymerization, estimates of k_D, k_{poly}, and f were required. The rate constants k_d and k_{poly} were measured by monitoring the concentration of initiator and monomer during polymerization using UV/vis absorption and ^{1}H NMR, respectively. The initiator was found to follow first-order kinetics while the polymerization of the monomer followed second-order kinetics, which are consistent with the simple model discussed above. At 82 °C, we determined k_D to be 1.15×10^{-4} s^{-1} and k_{poly} to be 2.59×10^{-3} M^{-1} s^{-1}.

The typical range for the initiator efficiency at different initiator concentration and reaction time was estimated by the ratio of the number of chains produced to the total amount of initiator radicals.

$$f = \frac{113([M]_0 - [M(t)])/M_n}{2[I_2]_0(1 - \exp(-k_D t))}$$

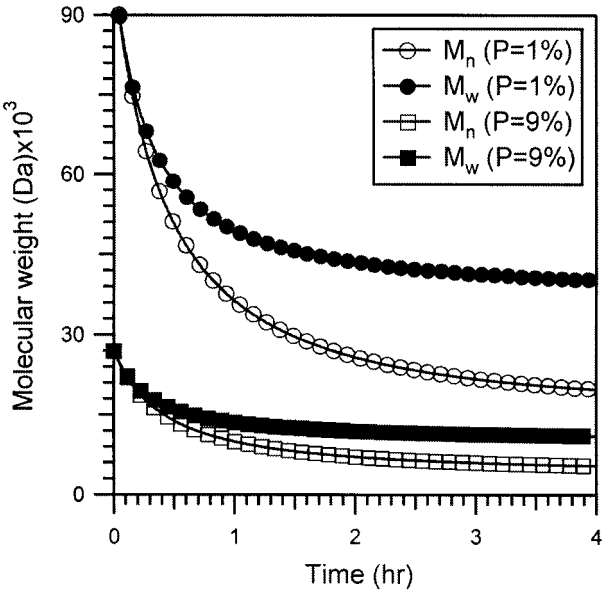

Figure 2. Calculated M_n and M_w as a function of polymerization time for two different ratios of initiator-to-monomer concentration.

Table 2. Comparison between Experimental and Predicted Molecular Weights

PNIPAM sample	M_n (kDa)	M_w (kDa)	f	$M_{n,predict}$ (kDa)	$M_{w,predict}$ (kDa)
P1T1	32.3	57.7	0.36	36.3	49.4
P1T4	21.7	36.6	0.29	19.7	40.2
P3T1	10.5	20.5	0.37	12.1	16.5
P3T4	7.8	17.5	0.27	6.6	13.4
P5T1	12.2	19.8	0.19	10.6	14.4
P5T2	6.8	16.5	0.24	7.5	12.7
P5T3	6.7	15.3	0.21	6.3	12.0
P5T4	5.1	14.4	0.25	5.7	11.7
P9T1	8.3	16.5	0.16	9.9	13.5
P9T4	6.5	13.9	0.11	5.4	11.0

Table 2 shows the calculated values of f for each PNIPAM sample based on the experimentally measured M_n. The calculated efficiency factors in Table 2 fall between 0.1 and 0.8 and are consistent with past studies for free-radical polymerization.[25] In general, the calculated f is inversely dependent upon the initial ACVA concentration; a slight effect of the time of reaction on f is also observed. The true value of f should be higher than values reported in Table 2 as the experimental estimates of M_n in Table 1 are high due to two reasons. First, the low sensitivity of the LS detector for short chains leads to a poorer estimation of M−H parameters for low molecular weights. Second, the samples in Table 1 have been dialyzed, and therefore, chains shorter than the molecular weight cutoff of the membrane do not contribute to the M_n.

The kinetic model was used to simulate the polymerization and to calculate M_n and M_w as a function of initiator concentration. For the kinetic calculations at each initiator concentration, an average f was used based on the values in Table 2.[26] Figure 2 shows the change in the calculated M_n and M_w as polymerization

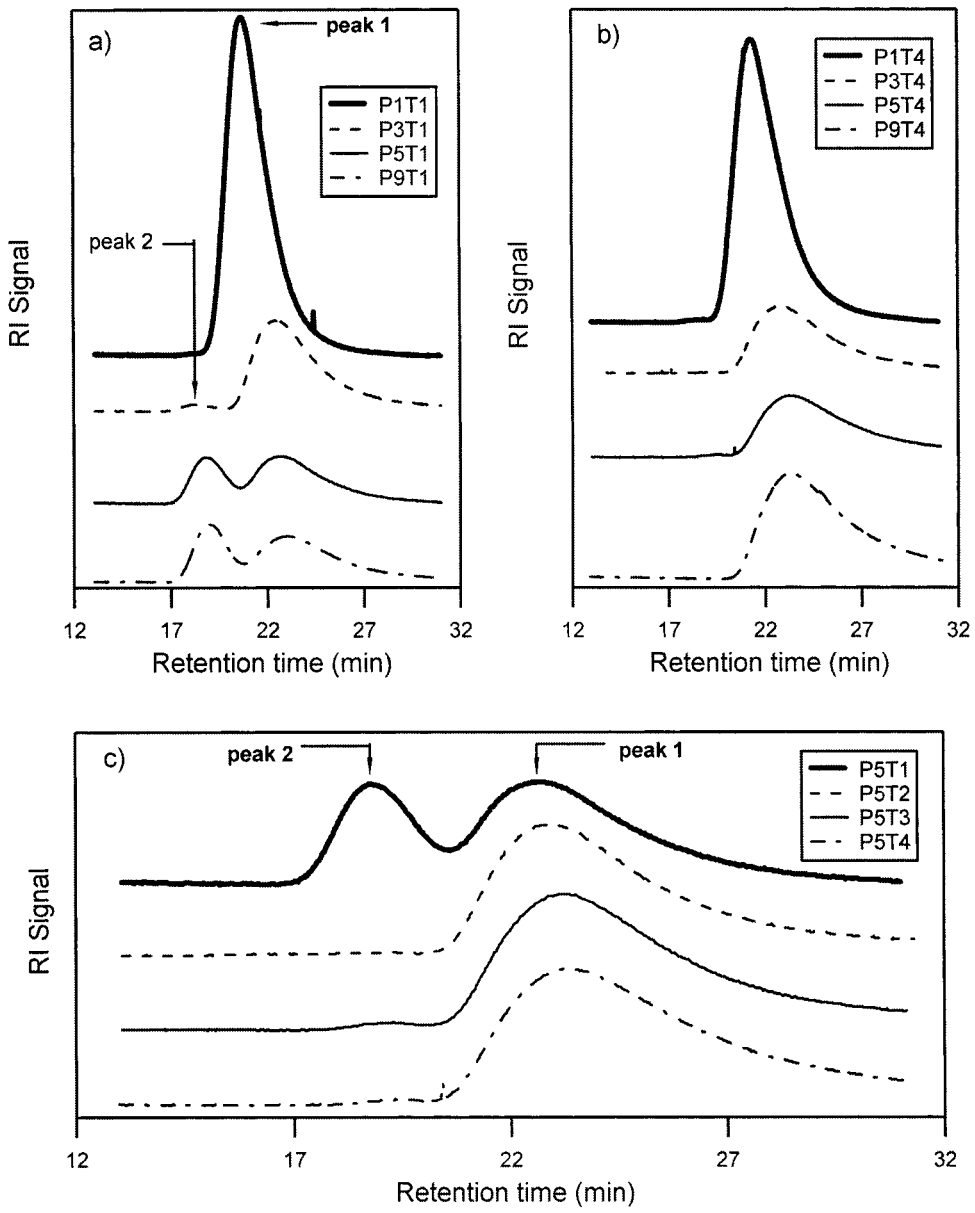

Figure 3. (a) Chromatogram of the refractive index (RI) detector signal for PNIPAM samples obtained after 1 h of polymerization. Total concentration of the samples injected in the column are 13.6 mg/mL (P1T1), 6.1 mg/mL (P3T1), 4.4 mg/mL (P5T1), and 5.4 mg/mL (P9T1). (b) Chromatogram of the refractive index (RI) detector signal for PNIPAM samples obtained after 4 h of polymerization. Total concentration of the samples injected in the column are 13.1 mg/mL (P1T4), 5.2 mg/mL (P3T4), 5.5 mg/mL (P5T4), and 9.0 mg/mL (P9T4). (c) Chromatogram of the refractive index (RI) detector signal for P5 samples after different polymerization times. Total concentration of the samples injected in the column are 4.4 mg/mL (P5T1), 4.7 mg/mL (P5T2), 5.2 mg/mL (P5T3), and 5.5 mg/mL (P5T4).

proceeds for two different initial ACVA concentrations. The kinetic model correctly predicts the trends for M_n and M_w with reaction time and initiator concentration. The predicted values for M_n and M_w that correspond to the experiments are shown in Table 2. Quantitatively, the average percent error between predicted and experimental values is lower for M_n (~13%) and higher for M_w (~19%) and is only slightly higher than the uncertainty in measurements of molecular weights.[27] The simple kinetic model, therefore, predicts M_n and M_w reasonably well.

Aggregation in Solution. Figure 3a shows the RI signal, which is proportional to mass concentration, for PNIPAM samples obtained after 1 h of polymerization (P1T1, P3T1, P5T1, P9T1). Except for the higher molecular weight material P1T1 all other samples exhibited two peaks: peak 1 at high retention times (~22 min) and peak 2 at short retention times (~18−19 min). The presence and location of peak 2 in the RI chromatogram indicates that the peak is due to either a fraction of very long chains giving a bimodal distribution or some kind of intermolecular association that leads to formation of aggregates which elute the column at short times.

Figure 3b shows the RI signals for the PNIPAM prepared using the same initiator concentration as shown in Figure 3a but after 4 h of polymerization (P1T4, P3T4, P5T4, P9T4). In this case none of the elution chromatograms show a second peak at low retention time. Figure 3c shows the elution chromatogram for P5 series of material wherein samples were withdrawn from the reaction mixture at four different times during the course of the reaction, purified, and then characterized. Interestingly, the RI signal for sample P5T1 obtained after 1 h shows two peaks that

are comparable in magnitude. However, the relative magnitude of peak 2 at short retention times decreases sharply for samples withdrawn at later stages in the polymerization. Peak 1 shifts slightly to higher retention times, which indicates the change in molecular weight distribution as shorter chains are produced.

Results in Figure 3b,c indicate that peak 2 in the RI signals is not due to a bimodal distribution of polymer chain lengths. Because a high molecular weight fraction cannot disappear during late stages of polymerization,[28] the presence of a peak indicates the presence of aggregates of polymer chains.[29] Surprisingly, the aggregation occurs in DMF even though it is a good solvent for poly(*N*-isopropylacrylamide) as indicated by the Mark−Houwink exponent of $a \sim 0.79$. The aggregates are observed at a fairly high temperature (60 °C) and at concentrations much lower than the overlap concentration ($C[\eta] \ll 1$; Table 1) of the polymer chains. Estimation of the peak areas shows that the aggregated fraction is 30−35% in both P5T1 and P9T1 but only ∼3−5% in P3T1.

Figure 3a shows that the retention time for peak 2 is quite similar in the different samples. Because the retention time depends on the hydrodynamic volume ($[\eta]M$) of the eluting species, this suggests that the aggregated structures possess similar size. By using the Einstein−Simha equation and the polystyrene calibration for $[\eta]M$, we estimated a sphere-equivalent hydrodynamic radius (R_h) for the different samples. The maximum of peak 2 in Figure 3a corresponds to $R_h \sim 18$ nm for P3T1 and $R_h \sim 11-12$ nm for P5T1 and P9T1. In contrast, the maximum of peak 1 for these three samples corresponds to $R_h \sim 2.2-2.5$ nm, which indicates that the aggregates are 5−7 times larger in size than the polymeric chains. Using the intrinsic viscosity measurement, the ratio M_{peak2}/M_{peak1} is approximately 30 for P3T1 and approximately 10−15 for P5T1 and P9T1.

We can also analyze the RALLS signal (R_{90^o}) for the samples shown in Figure 3 where $R_{90^o} = KCM_w$ is proportional to molecular (M_w) weight of the eluting species and its mass concentration (C). The RALLS signals for the samples obtained after 1 and 4 h of polymerization are shown in parts a and b of Figure 4, respectively. Figure 4c shows the RALLS signals for the series of PNIPAM-P5 samples that were withdrawn at different times during polymerization. All samples that showed the presence of a peak at short retention times (∼18−19 min) in the RI signal (Figure 3a) also showed a sharp peak in the RALLS signal (Figure 4a). In fact, the relative magnitude of the RI and RALLS signal for the two peaks in samples P5T1 and P9T1 indicates the disparity in molecular weights of the species that correspond to these two peaks. By using the peak maximum in the RI signal and the LS signal, the ratio M_{peak2}/M_{peak1} is approximately 28 for P3T1 and approximately 12−20 for P5T1 and P9T1, which agrees well with the estimates from the intrinsic viscosity and RI signal chromatogram.

For samples obtained after 4 h of polymerization, the RALLS signals (Figure 4b) show small secondary peaks at short retention times even though the corresponding RI signal in Figure 3b did not indicate any multiple peaks. These peaks in RALLS signal suggest traces of aggregated structures that are sometimes even larger (e.g., for sample P9T4) than those observed in Figure 4a. As in the case of RI signal (cf Figure 3c), Figure 4c shows that the RALLS signal corresponding to peak 2 for P5T1 also drops sharply as the polymerization time exceeds 1 h, which suggests once again the disappearance of the aggregation phenomena.

Our attempts to break up the aggregation were unsuccessful. Figure 5a shows the RI signals of the sample P9T1 in DMF when it was diluted 10-fold in concentration from 11.5 to 1.3 mg/mL. In all cases, the chromatogram showed the presence of peak 2 at the same retention time, ∼19 min. The ratio of areas of peak 1 to peak 2 was constant, indicating that the weight fraction of the aggregated material in the solution does not change. There was no shift in the retention time, which indicates that the hydrodynamic volume of the aggregates does not change appreciably. Interestingly, in the dilution runs the sample with a concentration of 11.5 mg/mL showed a third peak at ∼15 min in the RALLS signal that was reminiscent of the peak in sample P9T4 (cf. Figure 4b). Like P9T4, the RI signal indicated that the moieties giving rise to this peak were present in trace concentration. To test whether polar interactions were at play in the intermolecular association, the concentration of the salt LiBr was increased 4-fold to 0.2 M, but no effect was observed in the chromatogram. Preheating the sample to 45 °C prior to injection in the chromatographic column or performing the chromatography at 70 °C (Figure 6) also did not disrupt the aggregation.

To obtain insight into the aggregation phenomena, three results can be considered. First, as shown in Figure 3, the phenomenon largely disappeared for samples produced with reaction times greater than 1 h. This observation suggests that short polymer chains that are produced as the polymerization proceeds do not show significant aggregation. Second, we analyzed the PNIPAM in the aqueous supernatant obtained from centrifuging during the PNIPAM purification procedure. A sample P5T1-sup was recovered from the supernatant solution of sample P5T1 by evaporation of water. Figure 5b shows a comparison between the RI signals of the two samples. The molecular weight of P5T1-sup is smaller than P5T1 as evident by the shift to higher retention time. Molecular weight analysis showed that the polymer from the supernatant solution had $M_n \sim 6.6$ kDa and $M_w \sim 11.3$ kDa. More importantly, no sign of aggregation was observed for P5T1-sup. This difference also indicates that very low molecular weight species in the polymer mixture do not participate in aggregation. Finally, even though the P1T1 sample was obtained after reaction for 1 h, aggregation was largely absent from its RI signals (cf. Figure 3a). Its molecular weight of $M_n \sim 32.3$ kDa is substantially higher than the other samples that were obtained after a polymerization time of 1 h and that exhibited multiple peaks in their chromatogram. This result suggests that polymer chains lying in an intermediate molecular weight range are susceptible to intermolecular association. Among the samples in this study, the polymers with M_n between approximately 8.3 and 12.2 kDa exhibited aggregation (Figure 3).

What Causes Aggregation? Complex aggregation behavior of another water-soluble polymer, poly(ethylene oxide), in good solvents such as methanol, acetonitrile, chloroform, etc., has been reported and has been a subject of controversy.[30] Past researchers have speculated that the aggregation of PEO is a result of residual water in the solutions or hydrogen-bonding interactions.

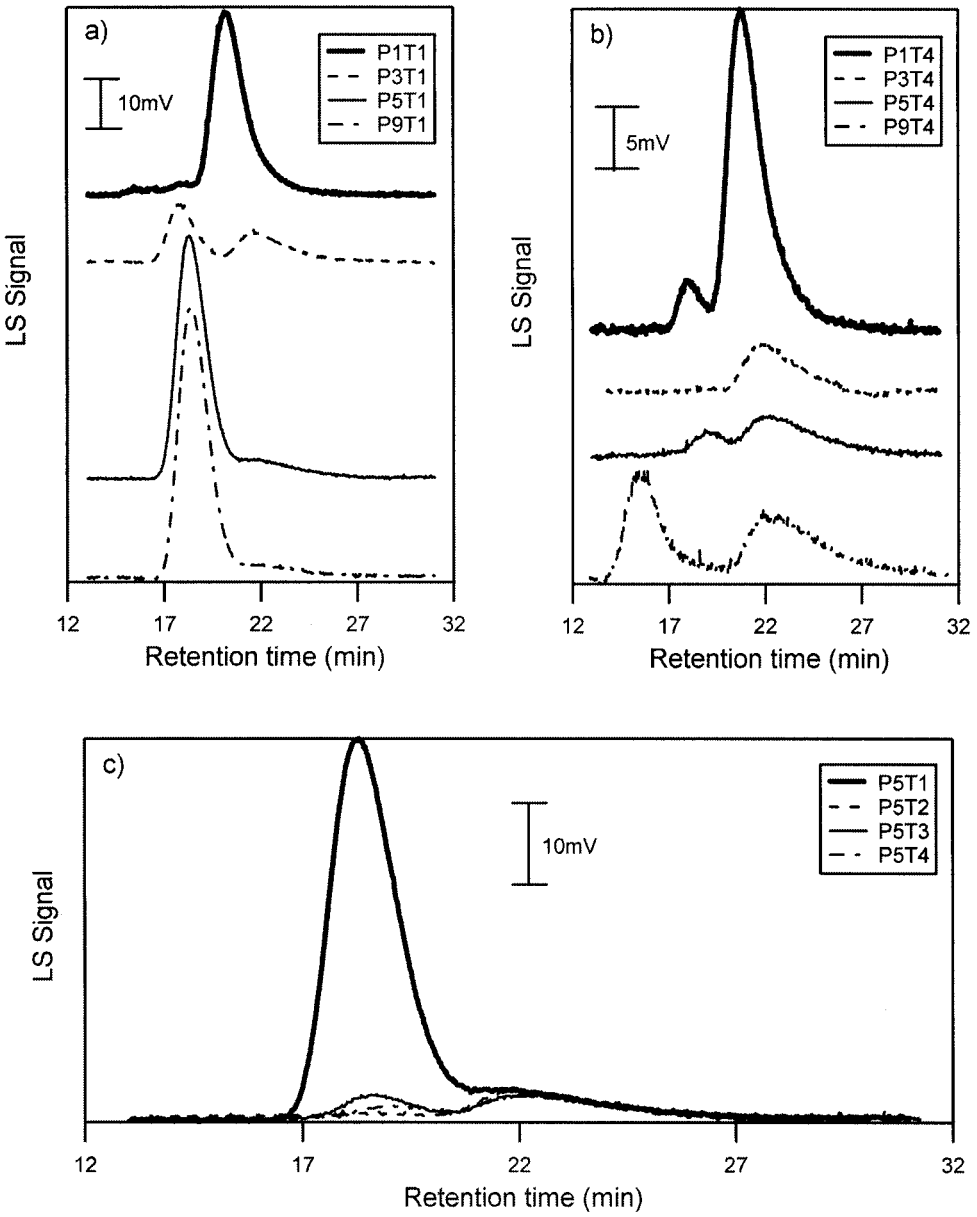

Figure 4. (a) Light scattering (LS) detector signal for PNIPAM samples obtained after 1 h of polymerization. (b) Light scattering (LS) detector signal for PNIPAM samples obtained after 4 h of polymerization. (c) Light scattering (LS) detector signal for P5 samples after different polymerization times.

Recent results by Duval and co-workers[31] support neither these speculations nor the aggregation due to impurities. Duval et al. suggest that PEO aggregates are a result of the history of preparation of the sample and that exposure of PEO to water at high temperatures greater than 89 °C but lower than the critical solution temperature (~102 °C) of PEO correlates with the observation of irreversible aggregation. In contrast to PEO, all samples of the telechelic PNIPAM studied here possess similar history in terms of the purification procedure, and yet only some samples show aggregation. Furthermore, aqueous solutions of PNIPAM are heated to 50−60 °C, which is above the LCST. The sample P5T1-sup that was recovered after evaporation of water also did not show aggregation. Because of these reasons, we believe that it is neither the history nor the drying after exposure to hot water that accounts for the presence of aggregation reported here.

Past studies on block copolymers (BCPs) have reported aggregation in dilute aqueous or organic solutions when the solvent is selective toward one block.[32,33] In the case of telomers, numerous studies have reported aggregation of hydrophobically modified polymers (HMPs) in aqueous solutions.[13,34,35] Aggregation of telechelic polymers in organic solutions has been observed only for polymers with ionic chain ends.[36,37] In all of these systems the classical picture of aggregation is one wherein the polymers form a micellar core of either hydrophobic alkyl chain ends (for HMPs) or one block of a copolymer (for BCPs). The core is protected by a shell of long, water-soluble chains or solvated blocks of BCPs.[32,35,38] The aggregation observed for the telechelic PNIPAM differs in several ways from these past studies, which makes direct analogy difficult. First, the carboxylic acid groups in the PNIPAM are not ionized. Second, high dielectric solvents such as DMF ($\epsilon \sim 36.7$) and elevated temperatures do not favor intermolecular association.[37,39] Third, while past studies[36,37] have suggested that the aggregation decreases with increase in molecular weight, an intermediate range of molecular

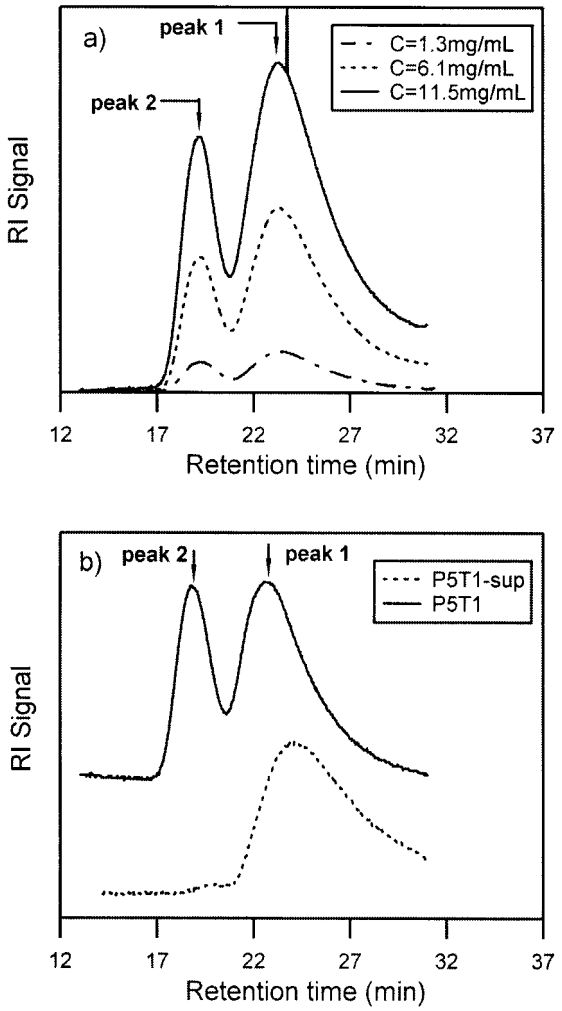

Figure 5. (a) Chromatogram of the refractive index (RI) detector signal for P9T1 sample illustrating the effect of bulk concentration. (b) Comparison of refractive index (RI) detector signal for P5T1 and the polymer recovered from the supernatant solution PNIPAM-P5T1-sup. See text for discussion.

weight for aggregation has not been observed. Fourth, in past reports the solvent either was nonselective for one of the polymer blocks or had unfavorable interactions with the chain ends in HMPs. In contrast, DMF is a good solvent for PNIPAM.

One characteristic of DMF that can underlie the interchain association is its hydrogen bond acceptor capability, which can lead to hydrogen bonds with carboxylic acid groups.[40] To test whether this characteristic is indeed important, the telechelic PNIPAM was studied in two other solvent systems using two different triple detector systems. Figure 6 shows the comparison of the RI chromatogram for P9T1 sample in DMF with the chromatogram in *N*-methylpyrollidone (NMP) and tetrahydofuran (THF). Like DMF, aggregation was also observed in the polar solvent NMP. As indicated by the areas of the peaks in Figure 6, the proportion of aggregates appears to change and there is a decrease in the fraction of aggregates. Interestingly, in THF no evidence of aggregation was observed. These results suggest that polar interactions are not the primary force driving aggregation as the polymers would be most susceptible to aggregation in the nonpolar THF (ϵ = 7.58) and not in the more polar NMP (ϵ = 32.2) or DMF (ϵ = 36.7). The chemical structures of the solvents indicate that differences exist in electron pair donor

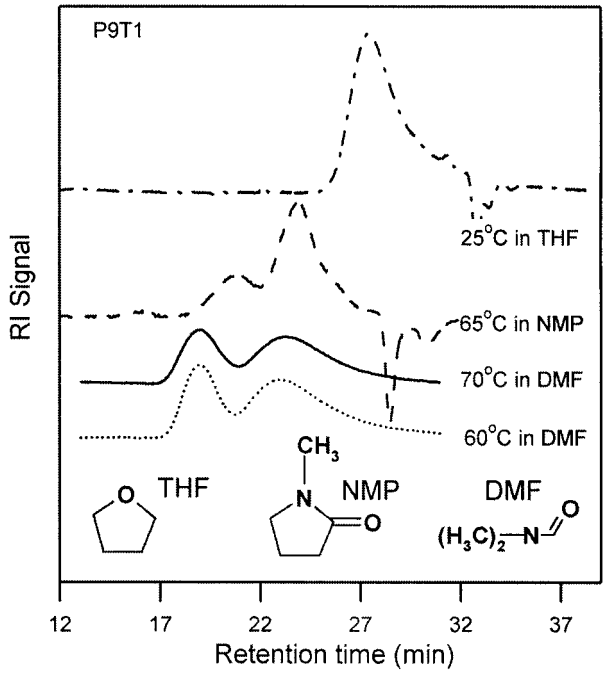

Figure 6. Chromatograms of the refractive index (RI) detector signal for P9T1 sample in DMF at 60 and 70 °C, NMP at 65 °C, and THF at 25 °C. The chemical structure of the solvents is shown in the inset.

ability (Lewis basicity) and the electron pair acceptor ability (Lewis acidity) of the three solvents. One common method to characterize these donor and acceptor capabilities relies on the Gutmann donor number (D_N) and acceptor number (A_N), respectively.[41] Indeed, THF has lower basicity and acidity (D_N = 20, A_N = 8) compared to those of DMF (D_N = 26.6, A_N = 16), and comparison of the aggregation phenomenon for the telechelic PNIPAM also reveals that the aggregation is absent in THF and highest in DMF. For NMP, which has intermediate values of D_N = 17 and A_N = 13.3, the degree of aggregation observed is larger than THF but lower than DMF. Thus, the effect of the solvent on the aggregation phenomenon indicates some type of solvent-mediated intermolecular association between the polymeric chains. However, the exact nature of this intermolecular interaction and the role of molecular weight of PNIPAM are unclear at this point and are the subject of our continuing investigation.

Conclusions

In conclusion, we have demonstrated the synthesis of telechelic poly(*N*-isopropylacrylamide) (PNIPAM) with carboxylic acid. Control over the molecular weight characteristics was possible by changing the monomer-to-initiator ratio and the time of polymerization. We interpreted the polymerization using a simple kinetic model based on decomposition of the initiator into radicals followed by initiation, propagation, and primary radical termination by initiator. Prediction of the molecular weights by this kinetic model showed good agreement with the experimentally observed values. Characterization of the polymer showed a complex aggregation phenomena in DMF solutions. For samples with M_n between 8.3 and 12.2 kDa the presence of large aggregates was evident in the elution chromatogram and the laser light scattering at 90°. The aggregation was irreversible, and neither dilution of the polymer nor addition of salt reduced reversed the association. The

aggregation phenomenon was also observed in another polar solvent (NMP) but not in THF, indicating that solvent molecules play a role in mediating the aggregation. The exact nature of the intermolecular association and the role of the molecular weight remain to be elucidated.

Acknowledgment. This research was carried out with the generous support of NSF (CAREER award CTS-9875467 to V.K.G.) and the University of Illinois. We thank William Shimer for assistance in the synthesis as part of his undergraduate research project.

References and Notes

(1) Pelton, R. *Adv. Colloid Interface Sci.* **2000**, *85*, 1−33. Gehrke, S. H. *Adv. Polym. Sci.* **1993**, *110*, 81−144. Irie, M. *Adv. Polym. Sci.* **1993**, *110*, 49−65.
(2) Galaev, I. Y.; Mattiasson, B. *Polym. Mater. Sci. Eng.* **1998**, *79*, 261−262.
(3) Okano, T. *Drug Delivery Syst.* **1995**, *10*, 355−361.
(4) Schild, H. G. *Prog. Polym. Sci.* **1992**, *17*, 163−249.
(5) Heskins, M.; Guillet, J. E. *J. Macromol. Sci., Chem.* **1968**, *2*, 1441−1455.
(6) Fujimoto, K.; Iwasaki, C.; Arai, C.; Kuwako, M.; Yasugi, E. *Biomacromolecules* **2000**, *1*, 515−518. Kurisawa, M.; Yokoyama, M.; Okano, T. *J. Controlled Release* **2000**, *69*, 127−137. Jeong, B.; Bae, Y. H.; Lee, D. S.; Kim, S. W. *Nature (London)* **1997**, *388*, 860−862. Shah, S. S.; Wertheim, J.; Wang, C. T.; Pitt, C. G. *J. Controlled Release* **1997**, *45*, 95−101. Yoshida, R.; Sakai, K.; Okano, T.; Sakurai, Y. *J. Biomater. Sci., Polym. Ed.* **1992**, *3*, 243−252.
(7) Yamamoto, K.; Kanazawa, H.; Matsushima, Y.; Takai, N.; Kikuchi, A.; Okano, T. *Chromatography* **2000**, *21*, 209−215. Teal, H. E.; Hu, Z.; Root, D. D. *Anal. Biochem.* **2000**, *283*, 159−165. Kanazawa, H.; Kashiwase, Y.; Yamamoto, K.; Matsushima, Y.; Kikuchi, A.; Sakurai, Y.; Okano, T. *Anal. Chem.* **1997**, *69*, 823−830. Freitas, R. F. S.; Cussler, E. L. *Sep. Sci. Technol.* **1987**, *22*, 911−919. Freitas, R. F. S.; Cussler, E. L. *Chem. Eng. Sci.* **1987**, *42*, 97−103.
(8) Chen, G.; Hoffman, A. S. *Bioconjugate Chem.* **1993**, *4*, 509−514. Liang, D.; Song, L.; Zhou, S.; Zaitsev, V. S.; Chu, B. *Electrophoresis* **1999**, *20*, 2856−2863. Takei, Y. G.; Matsukata, M.; Aoki, T.; Sanui, K.; Ogata, N.; Kikuchi, A.; Sakurai, Y.; Okano, T. *Bioconjugate Chem.* **1994**, *5*, 577−582. Kondo, A.; Kamura, H.; Higashitani, K. *Appl. Microbiol. Biotechnol.* **1994**, *41*, 99−105. Chen, G.; Hoffman, A. S. *Bioconjugate Chem.* **1993**, *4*, 509−514.
(9) Takei, Y. G.; Aoki, T.; Sanui, K.; Ogata, N.; Okano, T.; Sakurai, Y. *Bioconjugate Chem.* **1993**, *4*, 341−346. Takei, Y. G.; Aoki, T.; Sanui, K.; Ogata, N.; Okano, T.; Sakurai, Y. *Bioconjugate Chem.* **1993**, *4*, 341−346.
(10) Liang, L.; Feng, X.; Martin, P. F. C.; Peurrung, L. M. *J. Appl. Polym. Sci.* **2000**, *75*, 1735−1739. Suzuki, A. *J. Intell. Mater. Syst. Struct.* **1994**, *5*, 112−116.
(11) Bergbreiter, D. E. *Catal. Today* **1998**, *42*, 389−397.
(12) *Telechelic Polymers: Synthesis and Applications*; Goethals, E. J., Ed.; CRC Press: Boca Raton, FL, 1988. Velichkova, R.; Christova, D.; Panchev, I.; Gancheva, V. *NATO Sci. Ser., Ser. E* **1999**, *359*, 301−323. Van Caeter, P.; Goethals, E. J. *Trends Polym. Sci.* **1995**, *3*, 227−233. Jerome, R.; Henrioulle-Granville, M.; Boutevin, B.; Robin, J. J. *Prog. Polym. Sci.* **1991**, *16*, 837−906.
(13) *Water-Soluble Polymers: Synthesis, Solution Properties, and Applications*; Shalaby, S. W., McCormick, C. L., Butler, G. B., Eds.; ACS Symposium Series No. 467; American Chemical Society: Washington, DC, 1989.
(14) Ajaz, A. G. *Rubber Chem. Technol.* **1995**, *68*, 481−506.
(15) Geckeler, K. E.; Arsalani, N. *J. Macromol. Sci., Pure Appl. Chem.* **1996**, *A33*, 1165−1179. Geckeler, K.; Bayer, E. *Polym. Bull. (Berlin)* **1980**, *3*, 347−352. Hirao, A.; Hayashi, M. *Acta Polym.* **1999**, *50*, 219−231. Nuyken, O. *Angew. Makromol. Chem.* **1994**, *223*, 29−46.
(16) Takei, Y. G.; Aoki, T.; Sanui, K.; Ogata, N.; Okano, T.; Sakurai, Y. *Bioconjugate Chem.* **1993**, *4*, 42−46.
(17) Matsukata, M.; Takei, Y.; Aoki, T.; Sanui, K.; Ogata, N.; Sakurai, Y.; Okano, T. *J. Biochem.* **1994**, *116*, 682−686.
(18) Ohishi, H.; Nishi, T. *J. Polym. Sci., Part A: Polym. Chem.* **2000**, *38*, 299−309. Ohishi, H.; Ohwaki, T.; Nishi, T. *J. Polym. Sci., Part A: Polym. Chem.* **1998**, *36*, 2839−2847. Lebreton, P.; Boutevin, B. *J. Polym. Sci., Part A: Polym. Chem.* **2000**, *38*, 1834−1843. Lebreton, P.; Boutevin, B.; Gramain, P.; Corpart, J.-M. *Polym. Bull. (Berlin)* **1999**, *43*, 59−66.
(19) TriSEC GPC Version 3 Software Manual, Viscotek Corp., Houston, TX, 1999.
(20) Wang, P. J.; Glasbrenner, B. S. *J. Liq. Chromatogr.* **1988**, *11*, 3321−3333. *Detection and Data Analysis in Size Exclusion Chromatography*; Provder, T., Ed.; ACS Symposium Series No. 352; American Chemical Society: Washington, DC, 1987. *Chromatography of Polymers: Hyphenated and Multidimensional Techniques*; Provder, T., Ed.; ACS Symposium Series 731; American Chemical Society: Washington, DC, 1999. Yi, H.; Bu, L.; Bu, L.; Zhang, D.; Su, C.; Xu, Z.; Yip, L. W.; Tang, B.; Mays, J. W. *Polym. Bull. (Berlin)* **2000**, *44*, 539−546.
(21) Schild, H. G.; Tirrell, D. A. *J. Phys. Chem.* **1990**, *94*, 4352−4356.
(22) Dialysis of the polymer samples was necessary to remove ACVA. The dialysis markedly affected R_{COOH}, and it showed a rapid decrease from 13 to 15 to values close to 2 at which point changes in R_{COOH} remained small even after a prolonged period of dialysis.
(23) Termination of the polymer chains by combination of coupling and disproportionation is possible. The former will give a telechelic polymer with carboxylic acid end groups while the latter will lead to unsaturated chain ends. IR and NMR characterization of the purified polymer do not show double bonds, indicating that the extent of disproportionation is small, and suggest that the termination is dominated by the large amount of initiator in the reaction mixture.
(24) Odian, G. G. *Principles of Polymerization*; Wiley: New York, 1991.
(25) Corner, T. *Adv. Polym. Sci.* **1984**, *62*, 95−142.
(26) We chose the average value rather than a variable f for convenience as the goal of the calculations was to identify whether the kinetic model can be used as predictive tool for the molecular weight.
(27) We estimated the uncertainty in the molecular weight by characterizing a series of polystyrene narrow molecular weight standards with the TDA system. Comparison with the manufacturer supplied molecular weight (no error estimates provided) shows that the disagreement between the two values is typically 1−11% for M_w and 2−10% for M_n with the higher discrepancy when the samples have molecular weights smaller than 4000 and larger than 200 000. An upper bound of 10% was chosen for the uncertainty in the molecular weights reported in Table 1.
(28) PNIPAM is reported to have high thermal stability and TGA-FTIR results show that degradation occurs near 400 °C (see: Schild, H. G. *J. Polym. Sci., Part A: Polym. Chem.* **2000**, *38*, 1834−1843).
(29) The molecular weights reported in Table 1 correspond to the signal under peak 1 for all samples.
(30) Strazielle, C. *Makromol. Chem.* **1968**, *119*, 50−63. Carpenter, D. K.; Santiago, G.; Hunt, A. H. *J. Polym. Sci., Polym. Symp.* **1974**, *44*, 75−92. Polverari, M.; Vandeven, T. G. M. *J. Phys. Chem.* **1996**, *100*, 13687−13695.
(31) Duval, M. *Macromolecules* **2000**, *33*, 7862−7867. Duval, M.; Sarazin, D. *Polymer* **1999**, *41*, 2711−2716.
(32) Semenov, A. N.; Joanny, J. F.; Khokhlov, A. R. *Macromolecules* **1995**, *28*, 1066−1075. Balsara, N. P.; Tirrell, M.; Lodge, T. P. *Macromolecules* **1991**, *24*, 1975−1986. Bug, A. L. R.; Cates, M. E.; Safran, S. A.; Witten, T. A. *J. Chem. Phys.* **1987**, *87*, 1824−1833.
(33) Leibler, L.; Orland, H.; Wheeler, J. C. *J. Chem. Phys.* **1983**, *79*, 3550−3557.
(34) Shi, X.; Li, J.; Sun, C.; Wu, S. *Colloids Surf., A* **2000**, *175*, 41−49. Ringsdorf, H.; Venzmer, J.; Winnik, F. M. *Macromolecules* **1991**, *24*, 1678−1686. Yekta, A.; Xu, B.; Winnik, M. A. *NATO ASI Ser., Ser. E* **1996**, *327*, 319−330.
(35) Preuschen, J.; Menchen, S.; Winnik, M. A.; Heuer, A.; Spiess, H. W. *Macromolecules* **1999**, *32*, 2690−2695.
(36) Williams, C. E.; Russell, T. P.; Jerome, R.; Horrion, J. *Macromolecules* **1986**, *19*, 2877−2884. Timbo, A. M.; Higgins, J. S.; Peiffer, D. G.; Maus, C.; Vanhoorne, P.; Jerome, R. *J. Phys. IV* **1993**, *3*, 71−78. Bodycomb, J.; Hara, M. *Polym. Bull. (Berlin)* **1988**, *20*, 493−498.
(37) Zhong, X. F.; Eisenberg, A. *Macromolecules* **1994**, *27*, 1751−1758.
(38) Khalatur, P. G.; Khokhlov, A. R.; Kovalenko, J. N.; Mologin, D. A. *J. Chem. Phys.* **1999**, *110*, 6039−6049.
(39) Ying, Q.; Wu, G.; Chu, B.; Farinato, R.; Jackson, L. *Macromolecules* **1996**, *29*, 4646−4654.

(40) Hahn, S.-W.; Yun, Y.-K.; Jin, J.-I.; Han, O. H. *Macromolecules* **1998**, *31*, 6417−6425. Czugler, M.; Cserzo, M.; Weber, E.; Ahrendt, J. *J. Crystallogr. Spectrosc. Res.* **1991**, *21*, 501−505. Shi, L.; Wan, D.; Huang, J. *Macromol. Chem. Phys.* **2000**, *201*, 941−948. Liang, Y.-Z.; Li, Z.-C.; Li, F.-M. *J. Colloid Interface Sci.* **2000**, *224*, 84−90. Zhao, J. Q.; Pearce, E. M.; Kwei, T. K.; Jeon, H. S.; Kesani, P. K.; Balsara, N. P. *Macromolecules* **1995**, *28*, 1972−1978.

(41) Mayer, U.; Gutmann, V.; Gerger, W. *Monatsh. Chem.* **1975**, *106*, 1235. Gutmann, V. *The Donor−Acceptor Approach to Molecular Interactions*; Plenum Press: New York, 1978.

MA010769B